Pflugers Arch - Eur J Physiol (2015) 467:2473–2484
DOI 10.1007/s00424-015-1723-3

$Ca_V\beta_2$ transcription start site variants modulate calcium handling in newborn rat cardiomyocytes

Cristian Moreno[1] · Tamara Hermosilla[1] · Danna Morales[1] · Matías Encina[1] · Leandro Torres-Díaz[1] · Pablo Díaz[1] · Daniela Sarmiento[2] · Felipe Simon[2,3] · Diego Varela[1]

Received: 15 July 2015 / Accepted: 17 July 2015 / Published online: 12 August 2015

Abstract In the heart, the main pathway for calcium influx is mediated by L-type calcium channels, a multi-subunit complex composed of the pore-forming subunit $Ca_V1.2$ and the auxiliary subunits $Ca_V\alpha_2\delta_1$ and $Ca_V\beta_2$. To date, five distinct $Ca_V\beta_2$ transcriptional start site (TSS) variants ($Ca_V\beta_{2a\text{-}e}$) varying only in the composition and length of the N-terminal domain have been described, each of them granting distinct biophysical properties to the L-type current. However, the physiological role of these variants in Ca^{2+} handling in the native tissue has not been explored. Our results show that four of these variants are present in neonatal rat cardiomyocytes. The contribution of those $Ca_V\beta_2$ TSS variants on endogenous L-type current and Ca^{2+} handling was explored by adenoviral-mediated overexpression of each $Ca_V\beta_2$ variant in cultured newborn rat cardiomyocytes. As expected, all $Ca_V\beta_2$ TSS variants increased L-type current density and produced distinctive changes on L-type calcium channel (LTCC) current activation and inactivation kinetics. The characteristics of the induced calcium transients were dependent on the TSS variant overexpressed. Moreover, the amplitude of the calcium transients varied depending on the subunit involved, being higher in cardiomyocytes transduced with $Ca_V\beta_{2a}$ and smaller in $Ca_V\beta_{2d}$. Interestingly, the contribution of Ca^{2+} influx and Ca^{2+} release on total calcium transients, as well as the sarcoplasmic calcium content, was found to be TSS-variant-dependent. Remarkably, determination of atrial natriuretic peptide (ANP) and brain natriuretic peptide (BNP) messenger RNA (mRNA) abundance and cell size change indicates that $Ca_V\beta_2$ TSS variants modulate the cardiomyocyte hypertrophic state. In summary, we demonstrate that expression of individual $Ca_V\beta_2$ TSS variants regulates calcium handling in cardiomyocytes and, consequently, has significant repercussion in the development of hypertrophy.

Keywords Calcium transients · Auxiliary subunits · Cardiomyocytes · L-type calcium current

Introduction

L-type calcium channels (LTCCs) constitute the main Ca^{2+} influx pathway involved in the excitation–contraction coupling in cardiac muscle [2]. Ca^{2+} influx through these channels promotes opening of ryanodine receptors and the subsequent calcium release from sarcoplasmic reticulum. Thus, LTCCs help in establishing the rate and magnitude of the cardiac muscle contraction in a process named calcium-induced calcium release (CICR) [14]. In addition, Ca^{2+} influx trough LTCC is associated with intracellular signals that result in cardiac hypertrophy [18, 35], suggesting that either expression or changes in the activity of these channels may contribute to cardiac dysfunction.

Cardiac L-type Ca^{2+} currents are carried by a multi-subunit membrane complex that includes $Ca_V1.2$, as the pore-forming subunit that co-assembles with the auxiliary $Ca_V\alpha_2\delta_1$ and $Ca_V\beta$ subunits [32]. To date, four genes that encode the

Electronic supplementary material The online version of this article (doi:10.1007/s00424-015-1723-3) contains supplementary material, which is available to authorized users.

✉ Diego Varela
dvarela@bitmed.med.uchile.cl

[1] Centro de Estudios Moleculares de la Célula (CEMC), Programa de Fisiopatología, Facultad de Medicina, ICBM, Universidad de Chile, Santiago, Chile

[2] Departamento de Ciencias Biologicas, Facultad de Ciencias Biologicas and Facultad de Medicina, Universidad Andres Bello, Avenida Republica 239, Santiago, Chile

[3] Millennium Institute on Immunology and Immunotherapy, Santiago, Chile

$Ca_V\beta_{1\text{-}4}$ isoforms have been identified. At the functional level, they modify L-type Ca^{2+} current open probability and its activation and inactivation kinetics [5]. $Ca_V\beta_2$ is the most abundant isoform in the heart [23] with at least five variants ($Ca_V\beta_{2a\text{-}e}$). Such variants originate from distinct transcriptional starting sites (TSS) and therefore only differ in the composition and length of their N-terminal domain [17]. All five TSS variants are expressed in the adult heart [22, 34], with varying expression patterns during heart development and heart physiological state [4, 11, 24, 29, 19, 25].

In fact, while $Ca_V\beta_{2b}$ has a higher expression in the healthy heart, the $Ca_V\beta_{2a}$ TSS variant is found to be overexpressed in hypertrophy [24]. Furthermore, overexpression of the $Ca_V\beta_{2a}$ variant in the adult mouse heart is sufficient to induce, together with an enhanced L-type current, increases in peak Ca^{2+} transients and sarcoplasmic reticulum (SR) Ca^{2+} content [8]. These changes in the intracellular [Ca^{2+}], caused by $Ca_V\beta_{2a}$, are associated with the development of moderate cardiac hypertrophy, highlighting the relevance of the pattern of $Ca_V\beta$ TSS expression in the heart.

Overexpression of each $Ca_V\beta_2$ TSS variant in heterologous systems confers distinct biophysical properties to the L-type current, affecting mainly the inactivation rate and open probability of LTCC [22, 34], suggesting that cellular Ca^{2+} handling could depend on the $Ca_V\beta_2$ TSS variant expressed in the cardiomyocyte. However, the impact of $Ca_V\beta_2$ TSS variants on Ca^{2+} handling in cardiomyocytes has not been explored until now.

We have characterized $Ca_V\beta_2$ TSS variants present in neonatal rat cardiomyocytes, and with the use of recombinant adenoviruses, we have explored the impact of each $Ca_V\beta_2$ TSS variant on the endogenous L-type current and Ca^{2+} handling in neonatal cardiomyocytes. As expected, overexpression of $Ca_V\beta_2$ TSS variants increased L-type current density and produced distinctive changes on the activation and inactivation kinetics of the LTCC current that depended on the specific $Ca_V\beta_2$ TSS variants. Furthermore, intracellular calcium transient amplitudes induced by extracellular pulses were larger in cells overexpressing $Ca_V\beta_{2a}$, and smaller in cardiomyocytes transduced with $Ca_V\beta_{2d}$. Interestingly, the sarcoplasmic calcium content, as well as the partial contribution of Ca^{2+} influx versus sarcoplasmic reticulum Ca^{2+} release on total calcium transients, was found to be also dependent on the TSS variant expressed. As predicted, from the observed changes in Ca^{2+} homeostasis, cardiomyocyte hypertrophic state was clearly influenced by distinct $Ca_V\beta_2$TSS variants.

Methods

Isolation of cardiomyocytes

Rats were bred in the Animal Breeding Facility from the Facultad de Ciencias Químicas y Farmacéuticas, Universidad de Chile (Santiago, Chile). All studies were done with the approval of the Universidad de Chile Institutional Bioethical Committee. The method of isolation and cell culture is a variation of that described by Harary and Farley [20, 21]. Neonatal rats (post-natal day P0-1) were euthanized, and their heart and aorta were surgically excised. Once clean, hearts were minced in saline solution containing (in mM) 0.8 $MgS0_4$ ($7H_2O$), 116 NaCl, 5.4 KCl, 0.8 NaH_2PO ($4H_2O$), 5.6 glucose, and 20 HEPES (pH 7.4) to obtain a homogeneous suspension. Myocardial cells were dissociated by enzymatic digestion using a 3 U/ml papain and 0.2 mg/ml type II collagenase (Invitrogen) in a 100 μM $CaCl_2$, saline solution. Tissue pieces were incubated for 15 min at 37 °C under constant agitation. Thereafter, the supernatant was removed and the cells washed with saline solution (without $CaCl_2$) three to five times. The cells were then incubated (15 min at 37 °C, by agitation) in saline solution containing Ca^{2+} (1.2 mM), pancreatin (1.6 mg/ml, Sigma), and type II collagenase (0.2 mg/ml, Invitrogen). The supernatant was then withdrawn and centrifuged and the cells resuspended in DMEM (Invitrogen, Inc.0) supplemented with 10 % horse serum, 5 % fetal bovine serum (FBS), and 1 % antibiotic (Pen/Strept). This last step was repeated five times. Once collected, the cells were seeded on a culture plate and incubated for 3–4 h in an incubator (95 % O_2–5 % CO_2) at 37 °C to allow fibroblast adhesion. Subsequently, the supernatant was collected and centrifuged for 5 min at 900×*g*. The collected cells were resuspended in DMEM and seeded on gelatin (1 %) pre-treated plates. Sixteen hours later, the medium was replaced with DMEM plus 0.5 % FBS.

RT-PCR

Total RNA from primary cardiomyocytes was extracted using TRIzol® reagent (Life Technologies, Inc.) according to the manufacturer's directions. Samples were treated with DNAsaH I (Invitrogen, Inc.) before to complementary DNA (cDNA) synthesis to eliminate genomic DNA. Single-stranded cDNA was reverse transcribed from 200 ng total RNA by RT-PCR using the QPCR cDNA Synthesis Kit AffinityScript™ II (Stratagene Inc.) according to manufacturer's instructions.

Conventional PCR

One microliter of the cDNA reaction was used as template for the PCR. A common antisense primer $Ca_V\beta_{2AS}$ (cctgttgcatttgcagttcgga) was used in combination with TSS-$Ca_V\beta_2$ specific sense primers (expected band size is shown within parentheses): $Ca_V\beta_{2a}$ atgcagtgctgcgggctggtac (196 bp), $Ca_V\beta_{2b}$ atgcttgacaggcagttggtg (199 bp), $Ca_V\beta_{2c}$ atggaccaggcgagtggactgg (277 bp), $Ca_V\beta_{2d}$ atggtccaaagcgacacgtcc (349 bp), $Ca_V\beta_{2e}$

atgaaggccacctggatcaggc (217 bp), $28S_S$ gggtgttgacgcgatgtgat, and $28S_{AS}$ gaaaccacagccaagggaac. Thermal cycling parameters were as follows: 94 °C, 2 min; 35–40 cycles of 94 °C, 30s; 60 °C, 30 s; and 72 °C, 15 s. Final extension is at 72 °C for 5 min. PCR products were electrophoresed on 0.8 % agarose gels containing GelRed® (Biotium, Inc.). Specificity of each PCR product was confirmed by relative mobility of the predicted fragments for each variant. Amplified cDNAs were then purified (Gel Extraction Kit, Qiagen) and cloned into pGEM-T Easy vector® (Promega) for sequencing.

Semi-quantitative PCR

Real-time semi-quantitative PCR was performed using a Stratagene MX300P thermal cycler (Stratagene). PCR amplification of the 28S RNA was used as internal control. PCR reactions were done with Brilliant SYBR Green (Agilent technologies) according to the manufacturer's directions. In the preliminary studies, PCR products were subjected to agarose gel electrophoresis and melting curves to confirm amplification specificity. After setting the PCR protocol and confirming the identity of products, all subsequent PCR products were tested by melting curve to confirm amplification specificity. Results were analyzed according to the standard curve method (correlation coefficient ≥0.98) [27]. Specific mRNA abundance was calculated as the ratio of the specific mRNA amount relative to the amount of 28S within each sample, determined in duplicate. Primers used were the same as for conventional PCR except for the $Ca_V\beta_{2d}$ sense primer (aaagcgcggctcccg) and the common antisense primer (tcccggtcctcttccaaagaca). Exon3 (agactcctacaccagccgcc) was used to normalize the proportion of $Ca_V\beta_2$ TSS variants. For ANP amplification, primers used were as follows: ANPsense, tgagcgagcagaccgatgaag, and ANPas, gagcagagccctcagtttgctttt.

$Ca_V\beta_2$ TTS cloning

As the C-termini of all $Ca_V\beta_2$ splice variants are conserved, we used the $Ca_V\beta_{2a}$ (GeneBank #NM_053851) splice variant, previously cloned into the eukaryotic expression vector PMT and subcloned it into the adenoviral vector pAD/RFP (gift from Tong-Chuan He, Addgene plasmid # 12520), using DraI for $Ca_V\beta_{2a}$/PMT and EcoRV for pAD/RFP. Each TSS variant was amplified and cloned in pGEMT-easy vector, and the replacement of the N-terminal sequence for all $Ca_V\beta_2$ was done using NotI and EcoRV. Reverse primer for these experiments was ASEcoRV gcggaagttcagagtgaaatt. All isoforms were sequenced after being reconstituted.

Virus production

Adenoviral vectors were generated using the AdEasy system. Briefly, cDNAs of $Ca_V\beta_2$ TSS were subcloned into the commercial adenoviral vector pAD/RFP, and homologous recombination was done by PmeI linearized DNA transformation of BJ5183 cells. Recombinant adenoviral plasmids were digested with PacI and transfected in AdHek cells with Lipofectamine (Life Technologies) according to manufacturer guidelines. Following observation of cytopathic effects (CPEs; 14–21 days), cells were scrapped and subjected to three freeze–thaw cycles in dry-ice methanol bath. The resulting supernatant was used to infect a 10-cm dish of 90 % confluent AdHek cells. Following observation of CPEs after 2–3 days, viral particles were purified and expanded by infecting 10 plates of AdHek cells.

Cardiomyocytes infection

The number of viral particles for each adenovirus was determined by 260-nm absorbance and was in the order of 10^{11} particles per milliliter. In the preliminary experiments, appropriate infection level was determined by monitoring RFP fluorescence and cytopathic effects in cardiomyocytes infected with different virus titers; the effective virus titer was determined at 90 % infection efficiency (fluorescence) in the absence of cytopathic effects. Infection of cardiomyocytes was done at the moment of seeding in gelatin pre-treated plates by addition of the previously determined concentration of the respective adenovirus to DMEM medium supplemented with 10 % horse serum and 5 % fetal bovine serum (FBS). After 16 h, the medium was replaced with DMEM with 0.5 % FBS.

Electrophysiology and data analysis

Ba^{2+} currents were recorded by the perforated whole-cell patch clamp configuration using nystatin (final concentration of 2 μg/ml) [37]. Borosilicate glass pipettes were pulled to 2–4-MΩ resistance and filled with internal solution containing (mM) 108 CsCl, 4 $MgCl_2$, 2 $CaCl_2$, 10 EGTA, and 10 HEPES (pH 7.2 adjusted with CsOH); the bath solution contained (mM) 20 $BaCl_2$, 1 $MgCl_2$, 10 HEPES, 40 TEA-Cl, 10 glucose, and 65 CsCl (pH 7.2 adjusted with CsOH). Data were acquired at room temperature, using an Axopatch 200B amplifier and pClamp 8 software (Axon Instruments), low-pass-filtered at 5 kHz, and digitized at 10 kHz. Series resistance was compensated to 85 %. Data analysis, currents fitting, and offline leak subtraction were performed in Clampfit 8 (Axon Instruments), and all curves fitted with SigmaPlot 11 (Jandel Scientific). Current–voltage (I-V) plots were fitted using a modified Boltzmann equation:

$$I = \frac{G_{max} * (V - E_{rev})}{1 + e^{-(V - V_a)/k}}$$

where E_{rev} is the reversal potential, G_{max} is the maximum slope conductance, k is the slope factor, and V_a the half-activation voltage.

Calcium imaging

Plated cardiomyocytes were mounted in a perfusion chamber on the stage of an inverted microscope (Olympus IX-81, UPLFLN 40XO 40 ×/1.3 oil-immersion objective). Fluorescence was collected with a CCD-based imaging system (Olympus DSU) running CellR software (Olympus). Cells were incubated with Fura-2 AM or Fluo-4 (Molecular Probes; 1 mM) and then superfused for 10–20 min with a solution containing (mM) 100 NaCl, 5 KCl, 2 $CaCl_2$, 1 $MgCl_2$, 90 sorbitol, 5 glucose, and 10 HEPES, pH 7.4, adjusted with Tris. Fura-2 was alternately excited at 340 and 380 nm, and the fluorescence emitted at 510 nm was collected and recorded at 5 Hz. For Fluo-4, cells were excited at 480 nm, and the fluorescence emitted at 510 nm was collected and recorded at 10 Hz. For every experiment, signals were recorded and the background intensity subtracted, using a same-size region of interest outside the cells. Fura-2 results are expressed as the ratio between the 340- and 380-nm (340/380) signals. Fluo-4 results are expressed as normalized fluorescence (F/F0).

Western blot

Cells were lysed in cold hypotonic solution (50 mM TRIS, 1 % IGEPAL, 150 mM NaCl, 1 mM EDTA, pH 7.4, and protease inhibitors) for 1 h under constant agitation. Cell lysates were centrifuged at 13,000 rpm for 10 min. Proteins were separated by electrophoresis with 8 % SDS-PAGE gels for 3 h at 100 V and subsequently transferred to nitrocellulose membrane. $Ca_V\beta_2$ was identified using a polyclonal antibody (Alomone Cat.# ACC-105) and tubulin with a monoclonal antibody (Sigma-Aldrich Cat.# T5168). Proteins were visualized by ECL (Thermo Scientific).

Cardiomyocyte area determination

Cardiomyocytes infected with each TSS variant were visualized in an inverted microscope (Olympus IX81) 48 h after seeding in 35-mm glass coverslips. CCD camera images were acquired and cell area determination was performed offline using Image-J software. Transduced cells were identified by RFP fluorescence.

Statistics

Data are presented as means±SE. Statistical analysis of the data was performed with SigmaPlot 11 (Jandel Scientific) by unpaired Student's t test and was considered significant at $P<0.05$. One-way ANOVA test was performed for samples exposed to multiple treatments and was considered significant at $P<0.05$.

Results

Expression of $Ca_V\beta_2$ TSS variants in newborn rat cardiomyocytes

We studied the expression pattern of $Ca_V\beta_2$ TSS variants in primary cultures of newborn cardiomyocytes by end point PCR of isoform-specific amino-terminal primers (see the "Methods" section). As positive control, total RNA from juvenile rat left ventricle (1 month) was used. Each DNA fragment amplified was purified and sequenced. As seen in Fig. 1a, all but $Ca_V\beta_{2e}$ TSS were found to be expressed in newborn cardiomyocytes.

We next sought to establish the proportion of mRNA abundance between the different variants. To this end, semi-quantitative PCR was performed and mRNA abundance of each TSS variant was normalized by the total amount of TSS variants determined by the amplification of the first common exon (exon 3). As seen in Fig. 1, mRNA of $Ca_V\beta_{2b}$ is the most abundant in newborn (39±5 %), with the mRNAs of $Ca_V\beta_{2c}$ and $Ca_V\beta_{2d}$ being very abundant, corresponding to almost half of the mRNA TSS variants in neonatal cardiomyocytes (16±7 and 26±6 %, respectively, Fig. 1b). In contrast, juvenile (4-week) rat hearts show higher expression of the $Ca_V\beta_{2b}$ TSS variant (76±8 %) and a reduction in the expression level of $Ca_V\beta_{2c}$ (6±5 %) and $Ca_V\beta_{2d}$ (8±4 %) transcripts. Additionally, $Ca_V\beta_{2e}$ mRNAs are also found to be expressed in juvenile rat hearts, albeit at a relatively lower level (5±4 %). No significant changes were found for $Ca_V\beta_{2a}$ expression.

Alterations on $Ca_V\beta_2$TSS variants expression can importantly alter calcium homeostasis in the cardiomyocyte. Thus, we explored the effects on calcium handling upon differential overexpression of only those $Ca_V\beta_2$ TSS variants endogenously expressed in rat neonatal cardiomyocytes. We cloned and prepared recombinant adenoviral particles of each $Ca_V\beta_2$ subunit for expression in the aforementioned model, as it represents a robust and commonly utilized model in the study of endogenous L-type calcium channels. We pursue to contribute to the better understanding of how $Ca_V\beta$ subunits modulate calcium handling as this knowledge is incomplete.

As no specific antibodies for each variant are available, we could only corroborate total $Ca_V\beta_2$ protein overexpression. This was verified as early as 48 h post-infection (Fig. 1c). In RFP-infected cardiomyocytes, three bands of similar intensity were detected between 65 and 80 kD; note that the same pattern was observed in non-infected cardiomyocytes

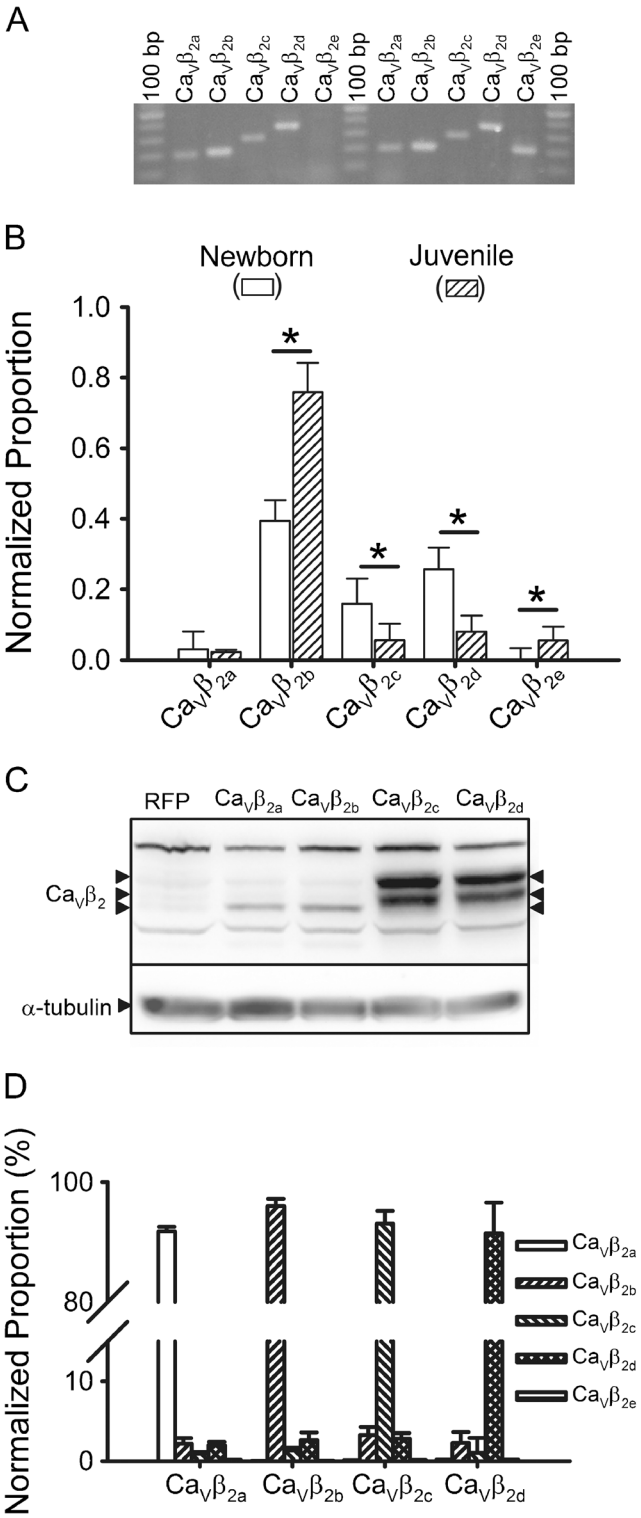

Fig. 1 Expression of $Ca_V\beta_2$ TSS variants in newborn rat cardiomyocytes and juvenile rat hearts. **a** Representative PCR-amplified $Ca_V\beta_2$ TSS variants from newborn rat cardiomyocytes (*left*) and juvenile rat hearts (*right*). **b** Bar graph (mean±sem) of semi-quantitative PCR expression for the five $Ca_V\beta_2$ TSS variants of mRNA isolated from newborn rat cardiomyocytes (n=5) (empty squares) or juvenile rat hearts (n=3) (hatched squares). **c** Western blot of 48-h infected newborn cardiomyocyte lysates probed with anti-CACNB2 antibody, showing marked overexpression of each $Ca_V\beta_2$ TSS variant when compared to endogenous $Ca_V\beta_2$ in RFP-infected cardiomyocytes (n=4). **d** Bar graph (mean±sem) of semi-quantitative PCR expression of the five $Ca_V\beta_2$ TSS variants. Total RNA isolated from cardiomyocytes 48 h post-infection with RFP or $Ca_V\beta_2$TSS variants found in newborn rat cardiomyocytes ($Ca_V\beta_{2a\text{-}d}$) (n=3 per variant). *P<0.05

(supplemental Fig. S1 for overexposed film). Infection with $Ca_V\beta_{2a}$ or $Ca_V\beta_{2b}$ constructs results in the relative increase in the lower molecular weight (MW) band intensity whereas $Ca_V\beta_{2c}$ or $Ca_V\beta_{2d}$ infection shows stronger intensity of the two higher MW bands, indicating that infection with each virus results in the overexpression of $Ca_V\beta_2$ protein. Semi-quantitative PCR was used to corroborate the expression of each specific $Ca_V\beta_2$ TSS variant construct. After 48 h of infection, over 90 % of the total $Ca_V\beta_2$ mRNA expressed in cultured cardiomyocytes corresponded to the exogenous variant overexpressed (Fig. 1d), without apparent changes in the relative proportion of $Ca_V\beta_2$ variants in cardiomyocytes upon RFP infection.

These results evidence that the levels of $Ca_V\beta_2$ variants expressed in newborn rat cardiomyocytes, in terms of the amount of mRNA copies, have an important contribution of $Ca_V\beta_{2c}$ and $Ca_V\beta_{2d}$. In parallel, we demonstrated the successful use of recombinant adenoviruses to achieve overexpression of exogenous $Ca_V\beta_2$ TSS variants in neonatal cardiomyocytes. Thus, we next focused in the functional consequences of each of the four $Ca_V\beta_2$ TSS variant overexpression on the endogenous L-type channel–mediated currents.

Endogenous L-type currents in cardiomyocytes infected with $Ca_V\beta_2$ TSS variants

Macroscopic Ba^{2+} currents were recorded from dispersed cardiomyocytes, expressing the corresponding $Ca_V\beta_2$ TSS variant or only RFP (Fig. 2a) with the nystatin perforated patch clamp method to ensure minimal disruption of the cytosolic environment; RFP reporter protein encoded by the adenoviral vector (independent CMV promoter) signaled positive infected cells; therefore, only bright red fluorescent cells were used. Adequate voltage control was verified by voltage-dependent Na^+ current measurements before each experiment [21]. Overexpression of all $Ca_V\beta_2$ TSS variants produced an increase in the mean current density at all voltages as seen in representative I-V plots from cells infected with each isoform compared to cells infected with RFP (Fig. 2b). Interestingly, the degree of current enhancement was dependent on the $Ca_V\beta_2$ variant that was overexpressed. The relative I_{max} increase (I_{TSS}/I_{RFP} at 0 mV) for each variant was $Ca_V\beta_{2a}$, 2.02±0.06; $Ca_V\beta_{2b}$, 1.51 ±0.10; $Ca_V\beta_{2c}$, 1.24±0.08; and $Ca_V\beta_{2d}$, 1.16±0.06 (Fig. 2c).

$Ca_V\beta_2$ TSS variants are known to alter L-type channel behavior, affecting activation as well as inactivation kinetics in heterologous expression systems [5]. Therefore, we

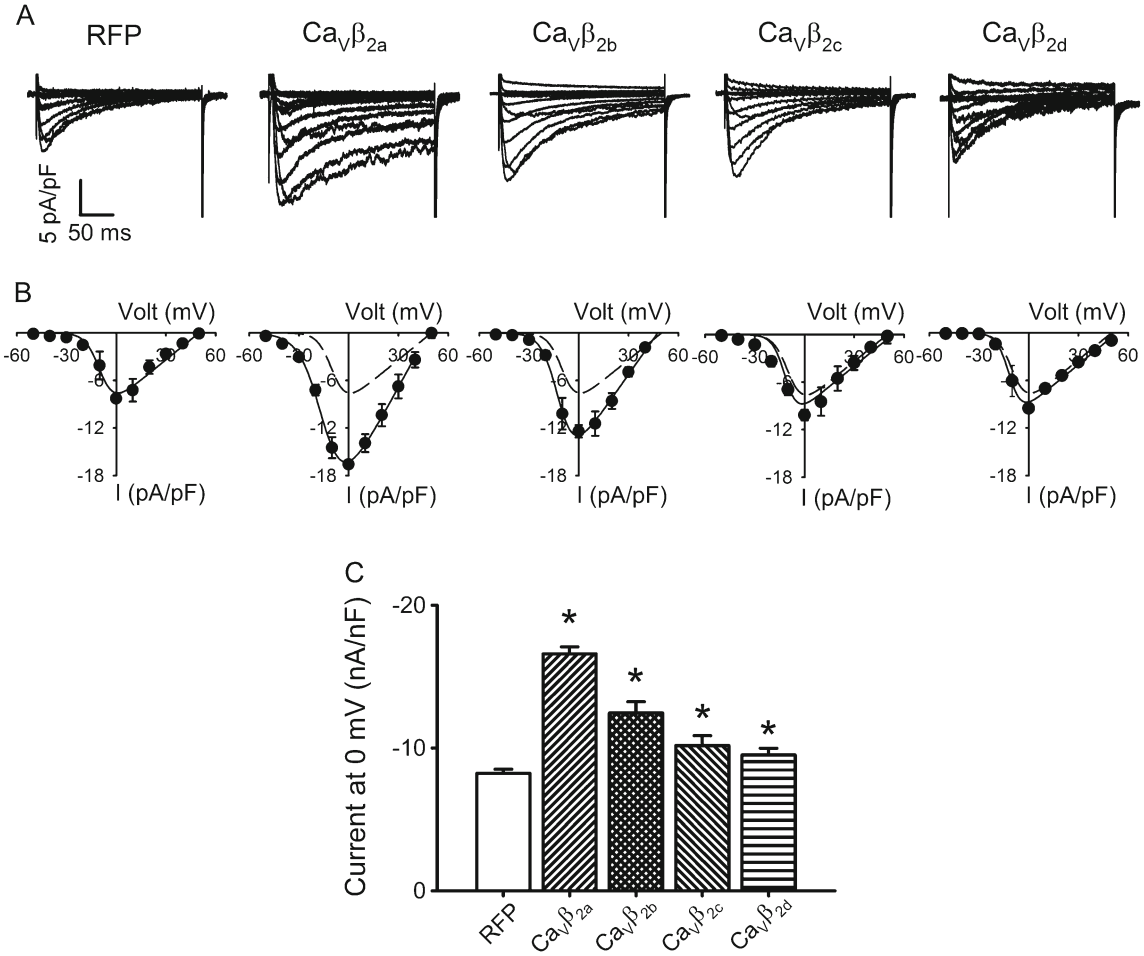

Fig. 2 Endogenous L-type currents from cardiomyocytes infected with different $Ca_V\beta_2$ TSS. **a** Representative nystatin-perforated whole-cell endogenous L-type Ba^{2+} current traces from cardiomyocytes infected for 48 h with different $Ca_V\beta_2$ TSSs. Currents elicited by a voltage step protocol from −60 to +50 mV in 10-mV increments, V_h=−80 mV. A 50-ms pre-pulse to −50 mV was applied to inactivate T-type calcium currents. **b** Summary peak current I/V plots (mean±sem) obtained from currents family as shown in (**a**); *black line* represents the best fit to a Bolztman equation (see the "Methods" section); for comparison, all plots include a *dashed line* from RFP-infected cardiomyocytes. **c** Bar graph (mean±sem) of the mean Ba^{2+} current obtained at 0 mV, normalized to the cell capacitance (n>6), *P<0.05 with respect to RFP

explored the effect of overexpression of each variant on endogenous L-type channel kinetics, as well as the RFP control group. The voltage dependence of activation was studied by single exponential fitting of the rising phase of current traces obtained at various potentials (Fig. 3a). Activation kinetics of RFP-infected cardiomyocyte Ba^{2+} currents showed shallow dependence on voltage, undistinguishable from those recorded in non-infected cardiomyocytes (not shown). In contrast, cardiomyocytes infected with $Ca_V\beta_{2a}$ exhibited slower activation (higher τ_{act}) at all voltages tested (−20 to 30 mV), with strong voltage dependence where the activation time constant became faster at depolarized potentials. On the other hand, $Ca_V\beta_{2b}$- and $Ca_V\beta_{2c}$-infected cardiomyocytes showed no significant activation kinetics difference when compared to RFP-infected cardiomyocytes. Finally, cardiomyocytes transducing $Ca_V\beta_{2d}$ displayed the similar voltage dependence as RFP-infected cardiomyocytes; however, faster kinetics were evident at all voltages tested (Fig. 3a).

L-type channel current inactivation kinetics were assessed by determining the residual current after a 250-ms pulse (R_{250}) at different voltage steps and plotted against the command potential. As seen in Fig. 3b, overexpression of $Ca_V\beta_{2a}$ affects significantly L-type channel inactivation in neonatal cardiomyocytes. Infection with $Ca_V\beta_{2b}$, $Ca_V\beta_{2c}$, and $CaV\beta_{2d}$ did not affect cardiomyocyte Ba^{2+} currents when compared to the RFP-infected controls.

Calcium transients in cardiomyocytes infected with $Ca_V\beta_2$ TSS variants

As one of the main effects of Ca^{2+} influx trough L-type calcium channels is the development of calcium transients, we proceeded to evaluate the effect of each TSS variant expression on calcium mobilization in cardiomyocytes.

Figure 4a illustrates representative intracellular calcium transient recording observed in cardiomyocytes transducing

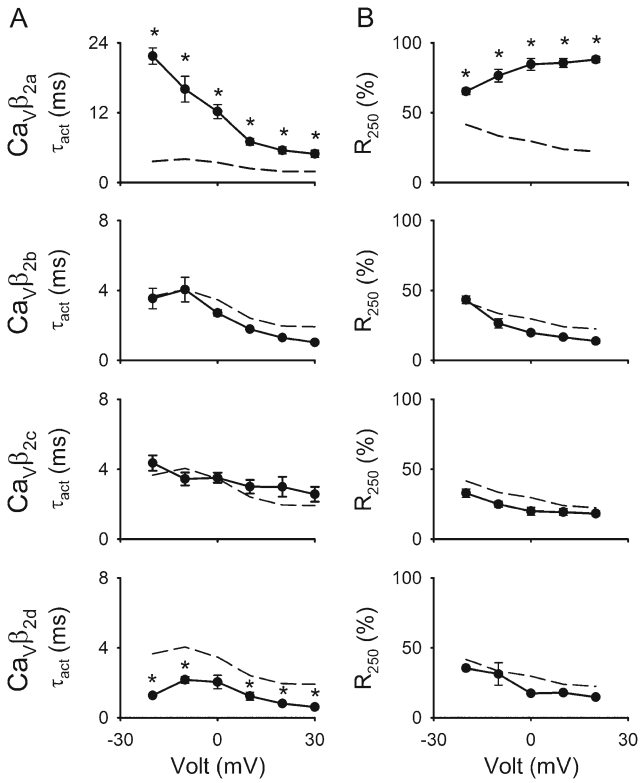

Fig. 3 Activation and inactivation kinetics of endogenous L-type currents from cardiomyocytes infected with different $Ca_V\beta_2$ TSS. **a** Voltage dependence of the activation time constant (τ_{act}, mean±sem) of LTCC from 48 h cardiomyocytes infected with each TSS variant. **b** Graph showing the residual of current after a 250-ms depolarization pulse (R_{250}, mean±sem) versus command voltage of L-type Ba^{2+} currents from $Ca_V\beta_2$ TSS–infected cardiomyocytes. Faster inactivation rates result in lower R_{250} values. In both panel sets, the *dashed line* represents RFP-infected cardiomyocytes data for comparison, ($n>6$) *$P<0.05$ with respect to RFP

each of the $Ca_V\beta_2$ TSS variants. Cells were loaded with Fura-2, and extracellularly paced by a 2-ms stimulus (frequency of 0.2 Hz). As shown, calcium transients from cardiomyocytes infected with $Ca_V\beta_{2b}$, $Ca_V\beta_{2c}$, or $Ca_V\beta_{2d}$ showed regular firing that was well coordinated with the external electrical stimulus. In contrast, $Ca_V\beta_{2a}$ infected cardiomyocytes displayed an irregular pattern evidencing calcium transients in between the pulses. A closer look of these inter-pulse calcium transients (supplemental movie 3) indicates that they likely correspond to calcium waves triggered after the initial calcium increase.

Two other observations can be drawn from the presented data so far: First, a faster time constant extracted from single exponential fits to the Ca^{2+}transient decay is evident in $Ca_V\beta_{2a}$ expressing cardiomyocytes, suggesting that intracellular calcium decrease is faster in these cardiomyocytes. Second, when compared to RFP-infected cardiomyocytes, calcium transient amplitudes from $Ca_V\beta_{2a}$, as well as $Ca_V\beta_{2b}$-infected cells, are larger while calcium transient amplitudes recorded from $Ca_V\beta_{2c}$- and $Ca_V\beta_{2d}$-infected cells are smaller (Fig. 4b). These data shows that although overexpression of $Ca_V\beta_{2c}$ or $Ca_V\beta_{2d}$ resulted in larger barium currents (Fig. 2c), the resulting calcium transients were smaller.

Moreover, diastolic calcium measurements indicate no differences in $Ca_V\beta_{2a}$- and $Ca_V\beta_{2b}$-infected cells. Nevertheless, they are smaller in cardiomyocytes bearing the $Ca_V\beta_{2c}$ or $Ca_V\beta_{2d}$ isoforms (Fig. 4d). This result is at variance with the observed maximal Ba^{2+} currents where, independent of the TSS variant infected, a larger current is recorded (Fig. 2b) and indicates that as in the case of $Ca_V\beta_{2a}$, other TSS variants induce bigger changes in calcium handling than the mere modification of L-type current.

Sarcoplasmic reticulum content in $Ca_V\beta_2$-TSS-infected cardiomyocytes

Calcium transients depend not only on calcium influx but also on the amount of calcium released from the sarcoplasmic reticulum (SR) by ryanodine receptor (RyR) activation, which is directly related with the total calcium stored in the sarcoplasmic reticulum. Cardiomyocytes from transgenic mice overexpressing $Ca_V\beta_{2a}$ show increased sarcoplasmic reticulum calcium content [10]. Thus, we explored whether $Ca_V\beta_2$ TSS overexpression produced variant-specific changes in the SR calcium content. To this end, infected cardiomyocytes were stimulated with a bolus of caffeine (10 mM) in the absence of extracellular calcium (plus 5 mM EGTA) to induce RyR opening and SR depletion (Fig. 5a).

The amplitude of caffeine-induced calcium increase is augmented in $Ca_V\beta_{2a}$-infected cardiomyocytes (Fig. 5b) but not affected by overexpression of $Ca_V\beta_{2b}$, $Ca_V\beta_{2c}$, or $Ca_V\beta_{2d}$. Moreover, they show that Ca^{2+} decay after the caffeine-stimulus has a faster time constant on those $Ca_V\beta_{2a}$-infected cardiomyocytes, while the Ca^{2+} decay is slower in $Ca_V\beta_{2c}$- and $Ca_V\beta_{2d}$-infected cardiomyocytes (Fig. 5c).

CICR in cardiomyocytes infected with $Ca_V\beta_2$ TSS variants

In freshly dissociated newborn cardiomyocytes, RyR-mediated CICR is estimated to be around 10 % of total calcium transient [13]; however, during culture, the RyR contribution to the calcium transient becomes larger [28]. In order to corroborate whether the $Ca_V\beta_2$ variants modify the CICR contribution to total calcium transients, changes in intracellular calcium were assessed before and 5 min after 50 μM ryanodine application. From those experiments, the difference within calcium transient amplitudes was calculated. To minimize fluorescent probe photo-bleaching, Fluo-4 was used and no signal was recorded during the 5 min of ryanodine exposure.

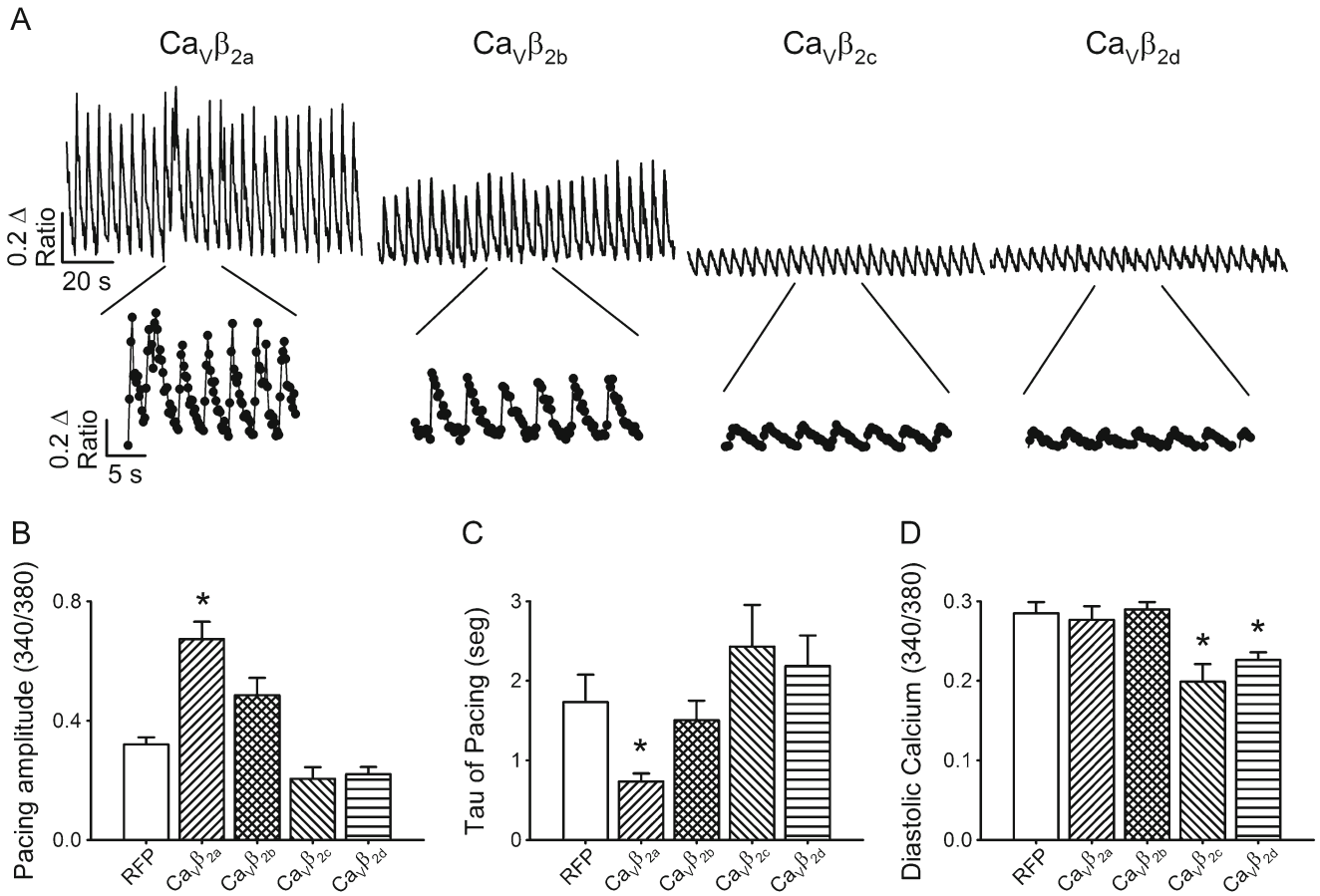

Fig. 4 Calcium transients in cardiomyocytes infected with $Ca_V\beta_2$ TSS variants. **a** Representative traces of 340/380 fluorescence ratio recordings from cardiomyocytes infected for 48 h with different $Ca_V\beta_2$ TSS and stimulated with a 2-ms external stimulus (0.2 Hz). Insets for each trace are shown below, individual points represent the signal for individual frames, acquired at 4 Hz. Bar graph (mean±sem) of average maximal amplitude of electrically evoked Ca^{2+} transients (**b**), time constant of Ca^{2+} decay (**c**), and resting Ca^{2+}(**d**) in cardiomyocytes infected for 48 h with different $Ca_V\beta_2$ TSS variants or RFP. Data obtained after fitting individual calcium transients to a single exponential (n>42, from 10 different cardiomyocyte preparations). *P<0.05 with respect to RFP

As summarized in Fig. 6b, the RyR contribution to calcium transients in rat neonatal cardiomyocytes infected with RFP, in our culture conditions, is considerably high (close to 80 %), and it is not affected by the overexpression of $Ca_V\beta_{2b\text{-}d}$. Interestingly, cardiomyocytes infected with $Ca_V\beta_{2a}$ showed a smaller contribution from RyR to calcium transients (Fig. 6a), indicating that calcium influx through L-type calcium channels is greater in cardiomyocytes that overexpress $Ca_V\beta_{2a}$.

Effect of $Ca_V\beta_2$ TSS variants on cardiomyocyte hypertrophy in vitro

The results presented so far demonstrate that $Ca_V\beta_2$ TSS variant expression distinctively modifies calcium handling. As Ca^{2+} homeostasis imbalances have been suggested to be a key player in the development of cardiac hypertrophy [30, 16], we next pursued to determine if $Ca_V\beta_2$ TSS variant overexpression could induce a hypertrophic phenotype in neonatal cardiomyocytes in vitro. To this purpose, the appearance of three different hypertrophic markers was determined in cardiomyocytes infected with each TSS variant: changes in cell area, and in the atrial natriuretic peptide (ANP) and brain natriuretic peptide (BNP) mRNA expression levels.

After 48 h of infection, the cell size of $Ca_V\beta_{2a}$-infected cardiomyocytes was 34±7 % larger than RFP-infected cardiomyocytes while infection with $Ca_V\beta_{2b}$ or $Ca_V\beta_{2c}$ did not induce perceptible changes in cell size. In contrast, overexpression of $Ca_V\beta_{2d}$ produced a modest but significant decrease in cell size (91±4 %, Fig. 7a). Concomitantly, ANP and BNP mRNA expression levels were increased in $Ca_V\beta_{2a}$ overexpressing cardiomyocytes but appear unchanged in $Ca_V\beta_{2b}$- or $Ca_V\beta_{2c}$-infected cardiomyocytes (Fig. 7b, c). It is worthy to observe that $Ca_V\beta_{2d}$ overexpressing cardiomyocytes resulted in reduced levels of ANP mRNA abundance but unchanged levels of BNP mRNA. Altogether, these data suggest that, under our experimental conditions, $Ca_V\beta_2$TSS variants distinctly modulate cardiomyocyte hypertrophy.

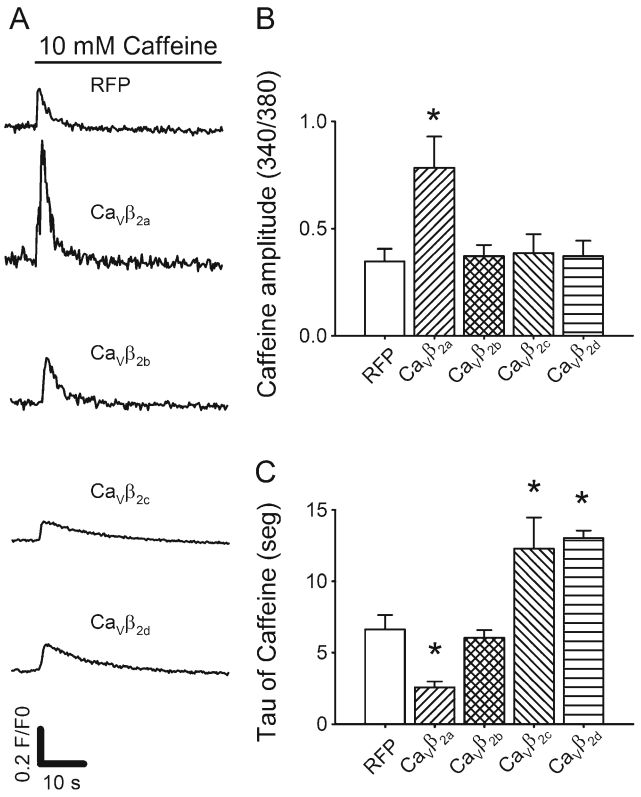

Fig. 5 Sarcoplasmic reticulum content in $Ca_V\beta_2$ TSS–infected cardiomyocytes. **a** Representative traces of 340/380 fluorescence ratio obtained from cardiomyocytes infected for 48 h with different $Ca_V\beta_2$ TSS. Stimulus consisted of a bolus of 10 mM caffeine in the absence of external calcium (5 mM EGTA). Acquisition frequency was 4 Hz. Bar graph (mean±sem) of average maximal Ca^{2+} response to a 10 mM caffeine bolus (**b**), or time constant of Ca^{2+} decay (**c**) in cardiomyocytes post-infection ($n>38$, from 10 different cardiomyocyte preparations).*$P<0.05$ with respect to RFP

Discussion

Our results show that about half of the $Ca_V\beta_2$ transcripts in newborn rat cardiomyocytes correspond to $Ca_V\beta_{2c}$ and $Ca_V\beta_{2d}$TSS variants (Fig. 1b). Concurrently, Western blots from neonatal cardiomyocyte lysates show three distinct bands of similar intensity. Multiple bands for $Ca_V\beta_2$ protein have been detected previously, and it is believed to be due to the expression of different variants. For instance, in mice cardiomyocytes, two bands have been detected, an ~68-kD band corresponding to $Ca_V\beta_{2b}$ and a $Ca_V\beta_{2d}$ of ~72 kD [25]. Consistent with this observation, our results show that overexpression of the shorter $Ca_V\beta_2$ TSS variants ($Ca_V\beta_{2a}$ or $Ca_V\beta_{2b}$) affects the apparent intensity of the lower MW band, while the overexpression of the longer variants ($Ca_V\beta_{2c}$ or $Ca_V\beta_{2d}$) similarly changes the relative intensity of the second and third band. The molecular basis for the two bands detected for the longer TSS variants has not been verified; however, it is likely related to post-translational modifications of the $Ca_V\beta_{2c}$ and $Ca_V\beta_{2d}$ variants that remain to be explored.

Even though we efficiently amplified and detected $Ca_V\beta_{2e}$ mRNA in juvenile rat hearts, no transcripts were detected in neonatal cardiomyocytes (Fig. 1a, b). This TSS variant has gained special attention together with $Ca_V\beta_{2a}$, as the only $Ca_V\beta$ subunits that are targeted to the plasma membrane, and confers slow inactivating kinetics to the L-type current in heterologous system [22, 26, 34]. Interestingly, a previous study in rats shows that $Ca_V\beta_{2e}$ is expressed in juvenile rat ventricles (4.5 weeks), but its expression is weak in 16-week-old animals [11]. Putting both results together demonstrates that $Ca_V\beta_{2e}$ TSS variant has a specific and time-dependent expression pattern. However, the physiological consequence of this phenomenon is yet to be explored.

The endogenous L-type calcium current modification observed after overexpression of $Ca_V\beta_{2c}$ and $Ca_V\beta_{2d}$ TSS variants indicates that on their own, such variants do not cause profound changes in whole-cell Ba^{2+} current kinetics when compared to $Ca_V\beta_{2b}$, the most abundant isoform expressed in newborn rat cardiomyocytes (Fig. 3). However, the maximal endogenous current is modified in a specific TSS variant manner (Fig. 2). As demonstrated previously, overexpression of $Ca_V\beta$ isoforms in adult cardiomyocytes increases the number of functional channels expressed in the plasma membrane [7]. This is achieved by at least two distinct mechanisms: (1) the binding of a deep hydrophobic region in $Ca_V\beta$ with the intracellular loop that links the domain I and domain II of $Ca_V1.2$ [36] that influences the rearrangement of the $Ca_V1.2$ intracellular regions [15] and increases the trafficking of $Ca_V1.2$ to the membrane, and (2) by preventing the targeting of $Ca_V1.2$ subunits to the endoplasmic reticulum–associated protein degradation (ERAD) complex [1]. Given that the interaction domain of $Ca_V\beta_2$ with $Ca_V1.2$ lies at the region where all $Ca_V\beta_2$ TSS variants are identical, it is unlikely that the $Ca_V\beta_2$ TSS variant differential effects we have shown are due to either of these mechanisms. It is thus plausible to hypothesize that the changes in maximal current we have observed could be related to changes in open probability. In fact, single-channel recordings of reconstituted L-type channels have demonstrated that $Ca_V\beta_{2c}$ and $Ca_V\beta_{2d}$ co-expression results in channels with the lowest open probability when compared to all other TSS variants known to date [22]. Consequently, increased expression of $Ca_V\beta_{2c}$ or $Ca_V\beta_{2d}$ may represent a novel mechanism for negative regulation of L-type calcium currents with unexplored therapeutic applications.

In addition, in the present study, we provide a systematic study of the effect of different $Ca_V\beta_2$TSS variants on calcium handling in neonatal rat cardiomyocytes. The main role of calcium influx through LTCC channels in normal excitation–contraction coupling has been well established [3], and its deregulation in pathological heart states, like hypertrophy, has been studied [9, 24, 29, 31]. Moreover, changes in calcium influx are enough to modify the activity of most proteins

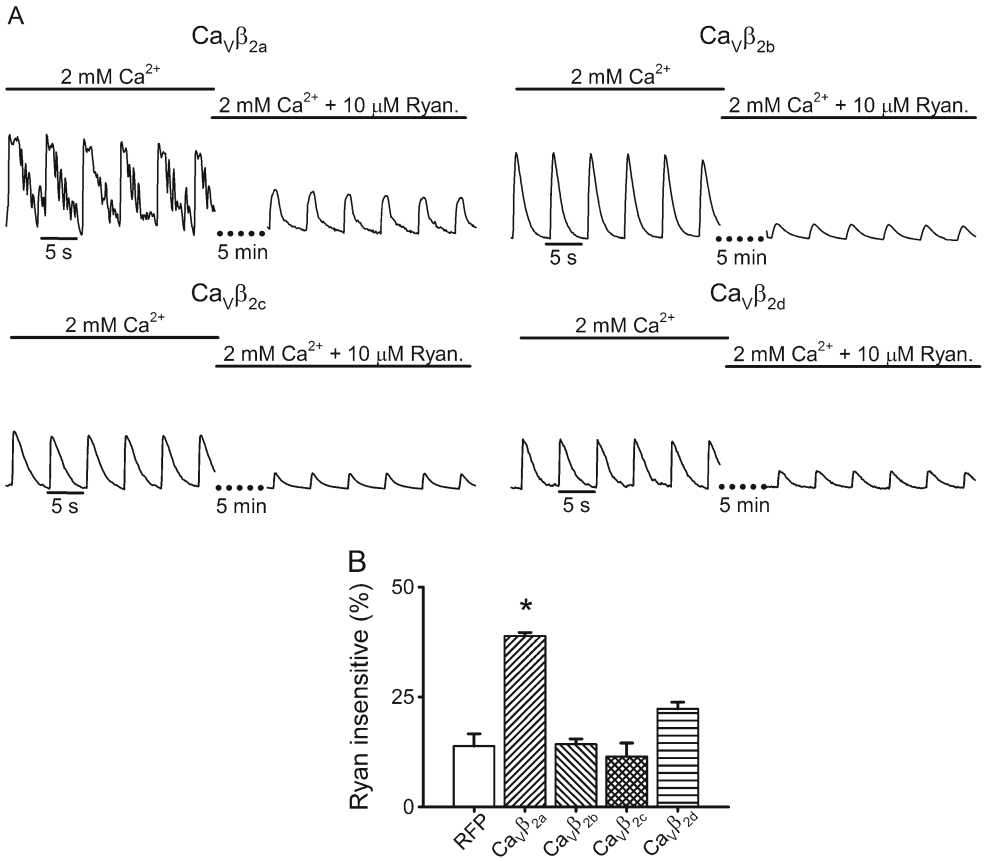

Fig. 6 CICR in cardiomyocytes infected with $Ca_V\beta_2$ TSS variants. **a** Normalized fluorescence (Fluo-4) traces recorded in cardiomyocytes infected for 48 h with different $Ca_V\beta_2$ TSS and stimulated with a 2-ms external electric field (0.2 Hz; 2 mM $[Ca^{2+}]_o$), before and after 10 μM ryanodine (Ryan) exposure. Every condition shows 30-s recording before Ryan treatment, and 30-s recording after 5 min of Ryan addition. Acquisition frequency was 10 Hz. **b** Percentage of remaining calcium transient after 5-min Ryan treatment ($n>60$ cell from eight different cardiomyocyte preparations) in cardiomyocytes infected for 48 h with different $Ca_V\beta_2$ TSS variants or RFP.*$P<0.05$ with respect to RFP

involved in calcium handling [4], although the mechanism is still unknown. For example, transgenic mice overexpressing the $Ca_V1.2$ subunit show only modest hypertrophy at 4 months of age. Together with an increased Ca^{2+} current, these animals show a significant modification in proteins responsible for calcium handling, including the upregulation of NCX activity, and an enhancement of SR-Ca^{2+} release and reuptake [33].

In this view, the role of $Ca_V\beta_{2a}$ in the development of hypertrophy is the most documented: Transgenic mice models demonstrate that overexpression of this variant augments the heart to body weight ratio and causes tissue fibrosis along with other hypertrophic markers [8]. Moreover, $Ca_V\beta_{2a}$ expression has been shown to increase in failing human hearts [24].

Our results support such body of data since the changes in calcium handling observed after 48 h of adenoviral infection containing $Ca_V\beta_{2a}$ TSS variant include (1) increased Ca^{2+} transient amplitude (Fig. 4b), (2) irregular calcium transient pattern with prevalent occurrence of inter-pulse spikes (Fig. 4a and supplemental movie 3), (3) higher amplitude of the caffeine-induced Ca^{2+} transient that correlates with a higher SR-Ca^{2+} load (Fig. 5b), and (4) a faster time constant for calcium removal, possibly related to higher NCX activity [12, 38] (Fig. 5c). In addition, the contribution of calcium influx to the overall calcium transient is augmented in the $Ca_V\beta_{2a}$ TSS variant cells (Fig. 6), probably as a consequence of the slow inactivation kinetics conferred by this subunit (Fig. 2b). These features suggest that $Ca_V\beta_{2a}$-infected cardiomyocytes have or will develop a hypertrophic phenotype, supported by the fact that these cardiomyocytes show increased cell area and expression of markers of pathological hypertrophy like an increase in ANP and BNP mRNA abundance, all in agreement with results from other groups [8].

Interestingly, the changes in intracellular calcium and hypertrophic state observed in $Ca_V\beta_{2a}$-infected cardiomyocytes cannot be exclusively attributed to an increase in LTCC current, as cardiomyocytes transduced with $Ca_V\beta_{2b}$ TSS variant showed increased Ba^{2+} current (Fig. 2) and augmented Ca^{2+} transient amplitude (Fig. 4b), when compared with RFP-infected cardiomyocytes. Nevertheless, in contrast to $Ca_V\beta_{2a}$-infected cardiomyocytes, those transduced with $Ca_V\beta_{2b}$ showed no changes in SR-Ca^{2+} load (Fig. 5b) or the calcium removal after caffeine stimulation time constant (Fig. 5c). Moreover, the calcium transients evoked in these cardiomyocytes were regular and coordinated with the extracellular stimulus (Fig. 4a and supplemental movie 2), and changes in cell area or expression of ANP or BNP mRNA levels were not detected. In any case, our results represent the cardiomyocyte state after 48 h of infection, and due to the higher L-type current observed, such cells can potentially follow a differentiation pathway related to the hypertrophic state.

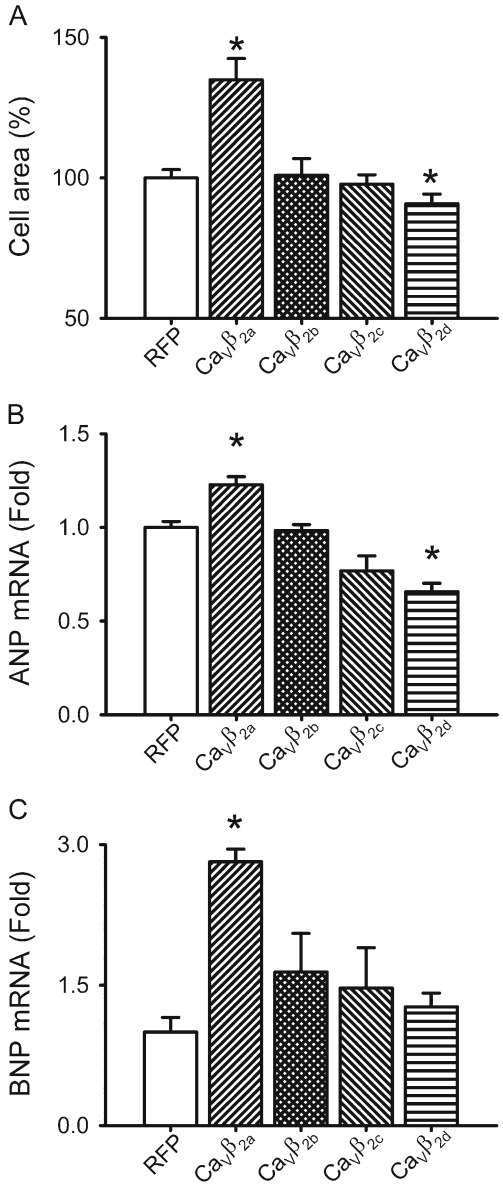

Fig. 7 Hypertrophic markers detected in $Ca_V\beta_2$ TSS variant–infected cardiomyocytes. **a** Bar graph (mean±sem) of cell area of cardiomyocytes infected with $Ca_V\beta_2$ TSS variants compared to RFP-infected cardiomyocytes (n>120 cell from 10 different cardiomyocyte preparations). **b** Bar graph (mean±sem) of semi-quantitative PCR expression for ANP mRNA from newborn rat cardiomyocytes after RFP or each $Ca_V\beta_2$ TSS variant infection (n=4). **c** Bar graph (mean± sem) of semi-quantitative PCR expression for BNP mRNA from newborn rat cardiomyocytes after RFP or each $Ca_V\beta_2$ TSS variant infection (n=4). *P<0.05 with respect to RFP

$Ca_V\beta_{2c\text{-}d}$-infected cardiomyocytes show only a modest increase in total Ba^{2+} current (Fig. 2), possibly as a consequence of a lower open probability [22]. Surprisingly, these cells have a smaller amount of diastolic calcium, and smaller calcium transient amplitude (Fig. 4b, d), in parallel with slower calcium removal after caffeine application (Fig. 5c), without changes in the SR content (Fig. 5b). Overall, these characteristics could reflect different sensitivities to hypertrophic stimulus in these cardiomyocytes as seen after $Ca_V\beta_2$ knockdown [6]. Indeed, cardiomyocytes are smaller after overexpression of $Ca_V\beta_{2d}$, and ANP mRNA abundance is reduced in these cardiomyocytes (Fig. 7). However, these observations have to be corroborated in whole animal model as previous reports have shown that a genetic reduction in L-type calcium current by partial deletion of CaCNA1C gene results in cardiac hypertrophy due to an increased neuroendocrine stimulation [18].

In summary, in this work, we have characterized the mRNA abundance of $Ca_V\beta_2$ TSS variants in newborn rat cardiomyocytes and their effect on endogenous L-type calcium current. Moreover, we demonstrate that, in terms of calcium handling, over-expression of $Ca_V\beta_{2a}$ (and probably $Ca_V\beta_{2b}$) is detrimental, and the overexpression of $Ca_V\beta_{2c}$ or $Ca_V\beta_{2d}$ seems to be beneficial. Our results strongly suggest that overexpression of these later variants of $Ca_V\beta_2$ should be explored as potential protectors against hypertrophic stimulus.

Acknowledgments We are thankful to Rocio K. Finol-Urdaneta, Andrés Stutzin, and Luis Michea for constructive discussion to the manuscript. This work was supported by research grants from Fondo Nacional de Desarrollo Científico y Tecnológico (Fondecyt) 1120240 to DV, and Fondecyt 1121078 and Millennium Institute on Immunology and Immunotherapy P09-016-F to FS.

Author's contributions D.V. and T.H. designed the project. C.M., T.H., L.T-D., D.M., M.E., P.D., D.S., and D.V. performed the experiments. D.V., T.H., and F.S. analyzed the data. D.V. wrote the manuscript.

Conflict of interest The authors declare no conflict of interests.

References

1. Altier C, Garcia-Caballero A, Simms B, You H, Chen L, Walcher J, Tedford HW, Hermosilla T, Zamponi GW (2011) The Cavbeta subunit prevents RFP2-mediated ubiquitination and proteasomal degradation of L-type channels. Nat Neurosci 14:173–180. doi:10.1038/nn.2712
2. Benitah JP, Alvarez JL, Gomez AM (2010) L-type Ca(2+) current in ventricular cardiomyocytes. J Mol Cell Cardiol 48:26–36. doi:10.1016/j.yjmcc.2009.07.026
3. Bers DM (2002) Cardiac excitation-contraction coupling. Nature 415:198–205. doi:10.1038/415198a
4. Bers DM (2006) Altered cardiac myocyte Ca regulation in heart failure. Physiology 21:380–387. doi:10.1152/physiol.00019.2006
5. Buraei Z, Yang J (2010) The beta subunit of voltage-gated Ca2+ channels. Physiol Rev 90:1461–1506. doi:10.1152/physrev.00057.2009
6. Cingolani E, Ramirez Correa GA, Kizana E, Murata M, Cho HC, Marban E (2007) Gene therapy to inhibit the calcium channel beta subunit: physiological consequences and pathophysiological effects in models of cardiac hypertrophy. Circ Res 101:166–175. doi:10.1161/CIRCRESAHA.107.155721
7. Colecraft HM, Alseikhan B, Takahashi SX, Chaudhuri D, Mittman S, Yegnasubramanian V, Alvania RS, Johns DC, Marban E, Yue DT (2002) Novel functional properties of Ca(2+) channel beta subunits

revealed by their expression in adult rat heart cells. J Physiol 541: 435–452
8. Chen X, Nakayama H, Zhang X, Ai X, Harris DM, Tang M, Zhang H, Szeto C, Stockbower K, Berretta RM, Eckhart AD, Koch WJ, Molkentin JD, Houser SR (2011) Calcium influx through Cav1.2 is a proximal signal for pathological cardiomyocyte hypertrophy. J Mol Cell Cardiol 50:460–470. doi:10.1016/j.yjmcc.2010.11.012
9. Chen X, Piacentino V 3rd, Furukawa S, Goldman B, Margulies KB, Houser SR (2002) L-type Ca2+ channel density and regulation are altered in failing human ventricular myocytes and recover after support with mechanical assist devices. Circ Res 91:517–524
10. Chen X, Zhang X, Kubo H, Harris DM, Mills GD, Moyer J, Berretta R, Potts ST, Marsh JD, Houser SR (2005) Ca2+ influx-induced sarcoplasmic reticulum Ca2+ overload causes mitochondrial-dependent apoptosis in ventricular myocytes. Circ Res 97:1009–1017. doi:10.1161/01.RES.0000189270.72915.D1
11. Chu PJ, Larsen JK, Chen CC, Best PM (2004) Distribution and relative expression levels of calcium channel beta subunits within the chambers of the rat heart. J Mol Cell Cardiol 36:423–434. doi:10.1016/j.yjmcc.2003.12.012
12. Dobrev D, Voigt N, Wehrens XH (2011) The ryanodine receptor channel as a molecular motif in atrial fibrillation: pathophysiological and therapeutic implications. Cardiovasc Res 89:734–743. doi:10.1093/cvr/cvq324
13. Escobar AL, Ribeiro-Costa R, Villalba-Galea C, Zoghbi ME, Perez CG, Mejia-Alvarez R (2004) Developmental changes of intracellular Ca2+ transients in beating rat hearts. Am J Physiol Heart Circ Physiol 286:H971–H978. doi:10.1152/ajpheart.00308.2003
14. Fabiato A (1983) Calcium-induced release of calcium from the cardiac sarcoplasmic reticulum. Am J Physiol 245:C1–C14
15. Fang K, Colecraft HM (2011) Mechanism of auxiliary beta-subunit-mediated membrane targeting of L-type (Ca(V)1.2) channels. J Physiol 589:4437–4455. doi:10.1113/jphysiol.2011.214247
16. Fatkin D, McConnell BK, Mudd JO, Semsarian C, Moskowitz IG, Schoen FJ, Giewat M, Seidman CE, Seidman JG (2000) An abnormal Ca(2+) response in mutant sarcomere protein-mediated familial hypertrophic cardiomyopathy. J Clin Invest 106:1351–1359. doi:10.1172/JCI11093
17. Foell JD, Balijepalli RC, Delisle BP, Yunker AM, Robia SL, Walker JW, McEnery MW, January CT, Kamp TJ (2004) Molecular heterogeneity of calcium channel beta-subunits in canine and human heart: evidence for differential subcellular localization. Physiol Genomics 17:183–200. doi:10.1152/physiolgenomics.00207.2003
18. Goonasekera SA, Hammer K, Auger-Messier M, Bodi I, Chen X, Zhang H, Reiken S, Elrod JW, Correll RN, York AJ, Sargent MA, Hofmann F, Moosmang S, Marks AR, Houser SR, Bers DM, Molkentin JD (2012) Decreased cardiac L-type Ca(2)(+) channel activity induces hypertrophy and heart failure in mice. J Clin Invest 122:280–290. doi:10.1172/JCI58227
19. Haase H, Pfitzmaier B, McEnery MW, Morano I (2000) Expression of Ca(2+) channel subunits during cardiac ontogeny in mice and rats: identification of fetal alpha(1C) and beta subunit isoforms. J Cell Biochem 76:695–703
20. Harary I, Farley B (1960) In vitro studies of single isolated beating heart cells. Science 131:1674–1675
21. Hermosilla T, Moreno C, Itfinca M, Altier C, Armisen R, Stutzin A, Zamponi GW, Varela D (2011) L-type calcium channel beta subunit modulates angiotensin II responses in cardiomyocytes. Channels 5: 280–286
22. Herzig S, Khan IF, Grundemann D, Matthes J, Ludwig A, Michels G, Hoppe UC, Chaudhuri D, Schwartz A, Yue DT, Hullin R (2007) Mechanism of Ca(v)1.2 channel modulation by the amino terminus of cardiac beta2-subunits. FASEB J Off Publ Fed Am Soc Exp Biol 21:1527–1538. doi:10.1096/fj.06-7377com
23. Hullin R, Khan IF, Wirtz S, Mohacsi P, Varadi G, Schwartz A, Herzig S (2003) Cardiac L-type calcium channel beta-subunits expressed in human heart have differential effects on single channel characteristics. J Biol Chem 278:21623–21630. doi:10.1074/jbc.M211164200
24. Hullin R, Matthes J, von Vietinghoff S, Bodi I, Rubio M, D'Souza K, Friedrich Khan I, Rottlander D, Hoppe UC, Mohacsi P, Schmitteckert E, Gilsbach R, Bunemann M, Hein L, Schwartz A, Herzig S (2007) Increased expression of the auxiliary beta(2)-subunit of ventricular L-type Ca(2)+channels leads to single-channel activity characteristic of heart failure. PLoS One 2, e292. doi:10.1371/journal.pone.0000292
25. Link S, Meissner M, Held B, Beck A, Weissgerber P, Freichel M, Flockerzi V (2009) Diversity and developmental expression of L-type calcium channel beta2 proteins and their influence on calcium current in murine heart. J Biol Chem 284:30129–30137. doi:10.1074/jbc.M109.045583
26. Miranda-Laferte E, Ewers D, Guzman RE, Jordan N, Schmidt S, Hidalgo P (2014) The N-terminal domain tethers the voltage-gated calcium channel beta2e-subunit to the plasma membrane via electrostatic and hydrophobic interactions. J Biol Chem 289:10387–10398. doi:10.1074/jbc.M113.507244
27. Pfaffl MW (2001) A new mathematical model for relative quantification in real-time RT-PCR. Nucleic Acids Res 29:e45
28. Poindexter BJ, Smith JR, Buja LM, Bick RJ (2001) Calcium signaling mechanisms in dedifferentiated cardiac myocytes: comparison with neonatal and adult cardiomyocytes. Cell Calcium 30:373–382. doi:10.1054/ceca.2001.0249
29. Schroder F, Handrock R, Beuckelmann DJ, Hirt S, Hullin R, Priebe L, Schwinger RH, Weil J, Herzig S (1998) Increased availability and open probability of single L-type calcium channels from failing compared with nonfailing human ventricle. Circulation 98:969–976
30. Semsarian C, Ahmad I, Giewat M, Georgakopoulos D, Schmitt JP, McConnell BK, Reiken S, Mende U, Marks AR, Kass DA, Seidman CE, Seidman JG (2002) The L-type calcium channel inhibitor diltiazem prevents cardiomyopathy in a mouse model. J Clin Invest 109:1013–1020. doi:10.1172/JCI14677
31. Shannon TR, Bers DM (2004) Integrated Ca2+ management in cardiac myocytes. Ann N Y Acad Sci 1015:28–38. doi:10.1196/annals.1302.003
32. Simms BA, Zamponi GW (2012) Trafficking and stability of voltage-gated calcium channels. Cell Mol Life Sci CMLS 69: 843–856. doi:10.1007/s00018-011-0843-y
33. Song LS, Guia A, Muth JN, Rubio M, Wang SQ, Xiao RP, Josephson IR, Lakatta EG, Schwartz A, Cheng H (2002) Ca(2+) signaling in cardiac myocytes overexpressing the alpha(1) subunit of L-type Ca(2+) channel. Circ Res 90:174–181
34. Takahashi SX, Mittman S, Colecraft HM (2003) Distinctive modulatory effects of five human auxiliary beta2 subunit splice variants on L-type calcium channel gating. Biophys J 84:3007–3021. doi:10.1016/S0006-3495(03)70027-7
35. Tandan S, Wang Y, Wang TT, Jiang N, Hall DD, Hell JW, Luo X, Rothermel BA, Hill JA (2009) Physical and functional interaction between calcineurin and the cardiac L-type Ca2+ channel. Circ Res 105:51–60. doi:10.1161/CIRCRESAHA.109.199828
36. Van Petegem F, Clark KA, Chatelain FC, Minor DL Jr (2004) Structure of a complex between a voltage-gated calcium channel beta-subunit and an alpha-subunit domain. Nature 429:671–675. doi:10.1038/nature02588
37. Varela D, Niemeyer MI, Cid LP, Sepulveda FV (2002) Effect of an N-terminus deletion on voltage-dependent gating of the ClC-2 chloride channel. J Physiol 544:363–372
38. Voigt N, Li N, Wang Q, Wang W, Trafford AW, Abu-Taha I, Sun Q, Wieland T, Ravens U, Nattel S, Wehrens XH, Dobrev D (2012) Enhanced sarcoplasmic reticulum Ca2+ leak and increased Na+-Ca2+ exchanger function underlie delayed afterdepolarizations in patients with chronic atrial fibrillation. Circulation 125:2059–2070. doi:10.1161/CIRCULATIONAHA.111.067306